Naval Research Laboratory

Washington, DC 20375-5000

NRL Memorandum Report 6500

The Dense Z-Pinch as a Plasma Radiation Source I. Quasi-Static Bennett Model

W. THORNHILL, J. L. GIULIANI, Jr. AND J. DAVIS

Plasma Radiation Branch
Plasma Physics Divison

July 10, 1989

This research was sponsored by the Defense Nuclear Agency, under Subtask Code and Title RL RA/Advanced Simulation Concepts, Work Unit Title, X-Ray Source Development Theory.

SECURITY CLASSIFICATION OF THIS PAGE

REPORT DOCUMENTATION PAGE

Form Approved
OMB No 0704-0188

1a REPORT SECURITY CLASSIFICATION UNCLASSIFIED	1b RESTRICTIVE MARKINGS
2a SECURITY CLASSIFICATION AUTHORITY	3 DISTRIBUTION / AVAILABILITY OF REPORT Approved for public release; distribution unlimited.
2b DECLASSIFICATION / DOWNGRADING SCHEDULE	
4 PERFORMING ORGANIZATION REPORT NUMBER(S) NRL Memorandum Report 6500	5 MONITORING ORGANIZATION REPORT NUMBER(S)
6a NAME OF PERFORMING ORGANIZATION Naval Research Laboratory 6b OFFICE SYMBOL (If applicable) Code 4720	7a NAME OF MONITORING ORGANIZATION
6c ADDRESS (City, State, and ZIP Code) Washington, DC 20375-5000	7b ADDRESS (City, State, and ZIP Code)
8a NAME OF FUNDING / SPONSORING ORGANIZATION Defense Nuclear Agency 8b OFFICE SYMBOL (If applicable) RAAEV	9 PROCUREMENT INSTRUMENT IDENTIFICATION NUMBER
8c ADDRESS (City, State, and ZIP Code) Alexandria, Virginia 22310	10 SOURCE OF FUNDING NUMBERS PROGRAM ELEMENT NO: 62715H; PROJECT NO:; TASK NO:; WORK UNIT ACCESSION NO: DN880-191

11 TITLE (Include Security Classification)
The Dense Z-Pinch as a Plasma Radiation Source I. Quasi-Static Bennett Model

12 PERSONAL AUTHOR(S)
Thornhill, W., Giuliani, J.L. Jr. and Davis J.

13a TYPE OF REPORT	13b TIME COVERED	14 DATE OF REPORT (Year, Month, Day)	15 PAGE COUNT
Interim	FROM _____ TO _____	1989 July 10	38

16 SUPPLEMENTARY NOTATION
This research was sponsored by the Defense Nuclear Agency, under Subtask Code and Title RL RA/Advanced Simulation Concepts, Work Unit Title, X-Ray Source Development Theory.

17 COSATI CODES		
FIELD	GROUP	SUB-GROUP

18 SUBJECT TERMS (Continue on reverse if necessary and identify by block number)
Bennett equilibrium
Dense Z-pinch
Fiber pinch
Radiation source

19 ABSTRACT (Continue on reverse if necessary and identify by block number)

The radiative yield from a slowly rising current, pulsed power driven, frozen deuterium z-pinch is investigated. This novel approach differs from the conventional z-pinch plasma radiation source which is driven by a rapid current rise leading to a fast implosion. The slow pinch is modeled as an adiabatic contraction subject to Bennett pressure equilibrium and driven by a constant generator voltage of 500 kV. Electron degeneracy effects are included in the pressure, but, the resistivity is taken as purely classical. The Bremsstrahlung radiation spectrum evolves from thin to nearly thick during the collapse phase. The present simple model predicts results that suggest that such plasmas may be useful as a Plasma Radiation Source.

20 DISTRIBUTION / AVAILABILITY OF ABSTRACT ☒ UNCLASSIFIED/UNLIMITED ☐ SAME AS RPT ☐ DTIC USERS	21 ABSTRACT SECURITY CLASSIFICATION UNCLASSIFIED
22a NAME OF RESPONSIBLE INDIVIDUAL Dr. Jack Davis	22b TELEPHONE (Include Area Code) (202) 767-3278 22c OFFICE SYMBOL Code 4720

DD Form 1473, JUN 86 *Previous editions are obsolete* SECURITY CLASSIFICATION OF THIS PAGE

S/N 0102-LF-014-6603

CONTENTS

THE DENSE Z-PINCH AS A PLASMA RADIATION SOURCE
I. QUASI-STATIC BENNETT MODEL

I. INTRODUCTION

This work is an extension of a previous investigation on the dynamics of a frozen deuterium fiber driven by a current pulse and has potential as a Plasma Radiation Source (PRS) for DNA applications. This radiation source is similar to those being used in the dense z-pinch experiments being undertaken at the Naval Research Laboratory[1] and Los Alamos National Laboratory[2]. Because of its similarity with the DZP work, we will refer to this source as a Dense Z-pinch Plasma Radiation Source (DZPRS). The DZPRS is a solid fiber of deuterium, although other materials can be used, that is heated and compressed using a long rise time current pulse. The long rise time allows the plasma to be slowly heated and compressed as compared to the impulsive heating and compression that occurs in a normal PRS. It is the purpose of this investigation to show that it may be more efficient to produce high energy radiation by heating and compressing in this manner. We employ Bennett hydrostatic equilibrium[3] in our model to simulate the DZPRS. The Bennett equilibrium model approximately includes electron degeneracy effects on the pressure. Furthermore, the model is self-consistently coupled to a circuit describing the pulse power generator. A description of the model and the results of a typical simulation are discussed in the following sections.

For conventional puff gas or wire array PRS schemes the load begins imploding at some distance from the axis, on the order of centimeters, and the current rise is fast, 10 - 100 kA/nsec. The kinetic energy rises with the current as the increasing J×B force does work on the plasma during the run-in phase. Then as the plasma begins to stagnate on axis, some of the stored kinetic energy is converted into internal energy by P-d(volume) work and shock heating. The result is a hot, highly ionized plasma which produces a radiation spectrum largely dependent upon the temperatures and densities achieved at stagnation. Zero- and 1-D PRS analyses show that there are two main requirements for producing radiation above the 1 keV range. First, there must be sufficient kinetic energy per ion to insure that large enough temperatures are obtained at stagnation, and secondly, the ion density has to be high so

Manuscript approved January 23, 1989.

that the plasma can efficiently radiate. Although a modest current is theoretically capable of heating a small load to the necessary temperatures, it cannot do this and at the same time push on enough mass to produce the ion densities needed for significant radiative emission. This theoretical result is supported by an experimental I^4 scaling law[4] observed for K-shell emission in Neon plasmas. (Note, in order to conserve energy, at high currents this scaling law must turn over and be less than or equal to I^2.) On the other hand, the K-shell emission might not be produced by direct conversion of kinetic energy into thermal energy as is proposed in the simple 0- and 1-D simulations. Rather it could arise from runaway electrons and hot spots generated by instabilities or other three-dimensional phenomena. The actual origin of the emission is still subject to theoretical and experimental investigation. From simple scaling arguments based on conventional z-pinch PRS loads, Apruzese and Davis[5] found that a 60 kJ yield from the K-shell of iron, which is in the 10 keV photon range, would require a superclass generator of 100 TW. Further analysis of the-state-of-the-art PRS sources can be found in the review by Pereira and Davis[6]. In lieu of a superclass device it is worthwhile to investigate alternative schemes such as the DZPRS.

The essential difference between the DZPRS and the PRS is that ion densities at implosion are much larger for the DZPRS. Densities are higher because the load is initially at solid state density and rapid shock heating is minimized. The longer rise time of the current pulse in the DZPRS leads to a gentler "cooking" and compression compared to the rapid implosion in a PRS. These conditions make it possible to keep the plasma in a quasi-equilibrium or Bennett-like state whereby the average particle pressure inside the plasma is in equilibrium with the magnetic pressure at the edge of the plasma. The evolution of the plasma is determined by slow changes in this equilibrium pressure. There are three mechanisms controlling the pressure. They are: 1) the ohmic heating rate, 2) the radiative cooling rate and 3) the rate of change of the current. If the radiative rates dominate then the plasma will collapse, hence the name "radiative collapse". In general the ohmic heating rate is larger than the radiative cooling rate until the time at which the current becomes greater than or equal to the "Pease-Braginskii" current[7]. There is experimental evidence to indicate that these plasmas remain stable while the current is rising: stable pinches have been observed for currents up to 640 kA[1]. If the DZPRS is found to be stable for higher currents and smaller line densities then have already been achieved, it will be possible to

obtain the temperatures and densities needed to produce significant radiation yields above 1 keV, as the plasma radiatively collapses. In this theoretical work we find that a deuterium plasma of 2×10^{18} cm^{-1} line density yields ~40 kJ of radiation above 3 keV while undergoing the radiative collapse.

II. MODEL EQUATIONS

A. Bennett Relation

To model the dynamics of a dense z-pinch undergoing a slow collapse we shall consider the simple case of a pinch with a uniform current density in Bennett equilibrium. Although such a pinch is in hydrostatic equilibrium, we will allow the plasma column to expand or contract in order to balance the resistive heating with the radiative cooling. Let $R_o(t)$ be the outer radius of the plasma column and $I(t)$ the current supplied by an external generator to the plasma load. For the assumed spatially uniform current density J_z along the z-axis one has

$$J_z(t) = \begin{cases} \dfrac{I(t)}{\pi R_o^2(t)} , & 0 \le r \le R_o; \\ 0 , & r \ge R_o . \end{cases} \tag{1}$$

From Ampere's law the azimuthal magnetic field B_ϕ is given by

$$B_\phi(r,t) = \begin{cases} \dfrac{r}{R_o(t)} B_o(t) , & 0 \le r \le R_o; \\ \dfrac{R_o(t)}{r} B_o(t) , & r \ge R_o ; \end{cases} \tag{2}$$

and $B_o = 2I/R_o c$ in cgs-gauss units where c is the speed of light. Note in these units the current I is in statamps [=statcoulomb/sec=$\sqrt{}$(ergs·cm/sec^2)]. The model of a uniform current and linear magnetic field inside the plasma column is valid as long as the time scale for magnetic diffusion through the whole plasma is small compared to the dynamic timescale.

In cylindrical symmetry the total momentum equation in the radial direction is

$$\frac{\partial \rho v}{\partial t} + \frac{1}{r}\frac{\partial}{\partial r}(r\rho v) + \frac{\partial}{\partial r}(p_i + p_e) = -\frac{1}{c} J_z B_\phi \,, \tag{3}$$

where ρ is the mass density, v the radial velocity, p_i the ion pressure, and p_e the electron pressure. The hydrostatic condition of Bennett equilibrium neglects the inertial terms and seeks a balance between the pressure forces and the current forces. This neglect is reasonable as long as the radial velocity is small compared to the plasma sound speed. Given the relations of eqns. (1) and (2), and the boundary condition of zero pressure at the outer plasma surface, one finds

$$p_i + p_e = \frac{I^2(t)}{\pi R_o^2(t) c^2}\left(1 - \frac{r^2}{R_o^2(t)}\right) . \tag{4}$$

Let N_l be the line density for the ions:

$$N_l \equiv \int_0^{R_o} n_i 2\pi r dr \,. \tag{5}$$

Furthermore, assume that the ion and electron temperatures are equal and uniform ($T_i = T_e = T$), that the mean charge state of the ions is also spatially uniform ($Z_i = n_e/n_i$), and that the plasma obeys the simple gas pressure formula. Equations (4) and (5) then lead to the classical Bennett relation:

$$N_l(1+Z_i)k_B T = \frac{I^2}{2c^2} \quad \Rightarrow \quad \frac{T}{eV} = 3.1\times10^3 \left(\frac{I}{MA}\right)^2 \left(\frac{1\times10^{18}\,cm^{-1}}{N_l(1+Z_i)}\right) . \tag{6}$$

The ion density follows from eqn.(4):

$$n_i(r,t) = \frac{2N_l}{\pi R_o^2(t)}\left(1 - \frac{r^2}{R_o^2(t)}\right) . \tag{7}$$

This density profile is consistent with the ion continuity equation as long as

$$v(r,t) = \frac{r}{R_o(t)} V_o(t) \,, \tag{8}$$

where $V_o = DR_o/Dt$ is the velocity of the outer radius. The velocity profile of eqn. (8) describes homologous motion of the plasma column.

Under some conditions the plasma column may collapse to such a small radius that electron degeneracy becomes important. To account for the degeneracy pressure in a simple manner we add the zero temperature Fermi pressure to the electron gas pressure:

$$p_e = n_e k_B T + \frac{2}{5} n_e \frac{h^2}{2m_e}\left(\frac{3n_e}{8\pi}\right)^{2/3} = n_e k_B T + \frac{2}{5} n_e k_B T_F(n_e) , \qquad (9)$$

where the Fermi temperature T_F is defined through the above relation and is a function of the electron density [$T_F(n_e) = (n_e/4.5\times10^{21}\text{cm}^{-3})^{2/3}$ eV]. If we use the average electron density $\bar{n}_e = Z_i N_l/\pi R_o^2$ to evaluate the Fermi temperature, the classical Bennett relation (6) is replaced by

$$N_l k_B T\left[1 + Z_i\left(1 + \frac{2}{5}\frac{T_F(\bar{n}_e)}{T}\right)\right] = \frac{I^2}{2c^2} , \qquad (10)$$

or

$$\frac{T}{eV} = \frac{3.1\times10^3}{(1+Z_i)}\left[\left(\frac{I}{MA}\right)^2\left(\frac{1\times10^{18}\text{cm}^{-1}}{N_l}\right) - Z_i^{5/3}\left(\frac{N_l}{1\times10^{18}\text{cm}^{-1}}\right)^{2/3}\left(\frac{1\times10^{-5}\text{cm}}{R_o}\right)^{4/3}\right]. \qquad (11)$$

Note that this revised relation requires a minimum current to support a Bennett pinch of a specified line density and radius. If the proper Fermi-Dirac integrals were used for the arbitrarily degenerate electron pressure instead of the approximation in eqn.(9), then a minimum current is also found. This latter approach, which requires extensive iteration for the degeneracy parameter, always leads to a positive pressure, unlike relation (11). For the present report we employ relation (11) and restrict our investigation to those solutions which maintain a positive temperature.

B. Dynamic Equation

So far we have adopted a uniform current density and employed the hydrostatic approximation in the momentum equation to obtain the classical Bennett relation for the plasma temperature in terms of the current and the

line density [eqn.(6)], we have found a quadratic profile for the plasma density assuming a spatially uniform temperature [eqn.(7)], and we have shown that a linear velocity law is consistent with the continuity equation [eqn.(8)]. The degeneracy pressure can be approximately included, leading to a revised Bennett relation [eqn.(11)]. We now turn our attention to the internal energy equation, which, in cylindrical symmetry, is given by

$$\frac{\partial}{\partial t}(\rho_i \varepsilon_i + \rho_e \varepsilon_e) + \frac{1}{r}\frac{\partial}{\partial r}[rv(\rho_i \varepsilon_i + \rho_e \varepsilon_e)] + (p_i + p_e)\frac{1}{r}\frac{\partial}{\partial r}(rv) + \frac{1}{r}\frac{\partial}{\partial r}[r(q_i + q_e)] = \eta_\perp J_Z^2 - \Lambda , \quad (12)$$

where $\eta_\perp$ is the perpendicular resistivity and Λ is the volumetric radiative cooling rate. By our previous assumption of a spatially uniform temperature the heat flux terms q_i and q_e can be dropped. For an ideal gas with a ratio of specific heat of $\gamma = 5/3$ we have

$$\rho_i \varepsilon_i + \rho_e \varepsilon_e = \frac{3}{2}(p_i + p_e) = \frac{3}{2} n_i k_B T\left[1 + Z_i\left(1 + \frac{2}{5}\frac{T_F(\bar{n}_e)}{T}\right)\right]. \quad (13)$$

As indicated by the last expression on the right hand side, the Fermi internal energy and pressure for the electrons at zero temperature likewise follow the ideal gas relation. The above profiles of eqns.(7) and (8) for the density and velocity are not necessarily consistent with the internal energy equation. Instead, we satisfy this equation in a global sense by integrating it over the plasma column. For an arbitrary function $f(r,t)$ we note the following relation:

$$\int_0^{R_o} \frac{\partial f(r,t)}{\partial t} 2\pi r dr = \frac{d}{dt}\int_0^{R_o} f(r,t) 2\pi r dr - f(R_o,t) 2\pi R_o V_o, \quad (14)$$

where d/dt is the Lagrangian time derivative following the plasma. Applying this operation to eqn.(12), using eqn.(7) for the density, eqn.(8) for the velocity, eqn.(13) for the pressure and internal energy, the generalized Bennett relation (10), and eqn.(1) for J_Z leads to

$$\frac{d}{dt}\left(\frac{3I^2}{4c^2}\right) + \frac{I^2}{c^2}\frac{V_o}{R_o} = \bar{\eta}_\perp \frac{I^2}{\pi R_o^2} - \frac{P_{rad}}{\Delta Z} , \quad (15)$$

where $\bar{\eta}_\perp$ is the spatial average of the electrical resistivity over the plasma column, $P_{rad} = \int \Lambda 2\pi r dr dz$, and ΔZ is the length of the plasma column along the z-axis. Equation (15) can be used to solve for the velocity of the outer radius of the plasma column:

$$\frac{dR_o}{dt} = V_o = \frac{c^2 R_o}{I^2} \left[\bar{\eta}_\perp \frac{I^2}{\pi R_o^2} - \frac{P_{rad}}{\Delta Z} - \frac{3}{4c^2} \frac{dI^2}{dt} \right] . \qquad (16)$$

Thus the dynamics of the plasma column is determined by the "p-d(volume)" work required to satisfy the internal energy equation (15). Under the condition that the velocity is small compared to the sound speed, one can neglect the kinetic energy equation. Note that radiative losses and an increasing current tend to constrict the plasma column, while resistive heating tends to expand it. The Pease-Braginskii current[7] I_{PB} is determined by balancing the resistive heating term against the radiative cooling term.

C. Circuit Model

The current I is determined by coupling the voltage drop across the plasma load (V_{load}) to a circuit equation describing the generator. Let the generator be characterized by a constant inductance (L_g), a constant resistance (Z_g), and a constant generator voltage (V_g). The equation for the circuit is simply

$$L_g \frac{dI}{dt} + Z_g I = V_g - V_{load} . \qquad (17)$$

We can determine the load voltage drop by looking at total plasma plus magnetic field energy conservation. The conservation relation for the field energy is given by Poynting's theorem:

$$\frac{\partial}{\partial t} \left(\frac{B_\phi^2}{8\pi} \right) - \frac{1}{r} \frac{\partial}{\partial r} \left(\frac{c}{4\pi} r E_Z B_\phi \right) = - J_Z E_Z , \qquad (18)$$

where E_Z is the z-component of the electric field. Applying an operation similar to eqn.(14) on the above equation we find

$$\frac{d}{dt}\int_0^{R_w}\left(\frac{B_\phi^2}{8\pi}\right)2\pi r dr dz - \left(\frac{B_\phi^2}{8\pi}2\pi r v \Delta Z\right)\Big|_0^{r=R_w} - \left(\frac{c}{4\pi} r E_Z B_\phi 2\pi \Delta Z\right)\Big|_0^{r=R_w} = -\int_0^{R_w} J_Z E_Z 2\pi r dr dz, \tag{19}$$

where R_w is a fixed radius outside of the plasma column. The first term can be broken into an integral over the plasma column (r=0 to $r=R_o$) and an integral over the surrounding vacuum region ($r=R_o$ to $r=R_w$). In these two regions B_ϕ is given by eqn.(2) and the integrals can be done explicitly. The second term vanishes because the velocity is zero at both boundaries. For the term on the right hand side the upper limit to the integral can be replaced by R_o since the current density is restricted to the plasma column. Within this region the electric field is given by

$$E_z = -\frac{v}{c} B_\phi + \eta_\perp J_z \,. \tag{20}$$

Using eqns.(1), (2), and (8) this integral over $\mathbf{J}\cdot\mathbf{E}$ can be performed. The result for the field energy equation is

$$\frac{d}{dt}\left(\frac{I^2}{4c^2}\right) + \frac{d}{dt}\left[\frac{I^2}{c^2}\ln\left(\frac{R_w}{R_o}\right)\right] - IE_Z(R_w) = \frac{I^2}{c^2}\frac{V_o}{R_o} - \bar{\eta}_\perp \frac{I^2}{\pi R_o^2} \,. \tag{21}$$

The first term is the time derivative of the magnetic field energy per unit length in the plasma column, the second term is the time derivative of the magnetic field energy per unit length in the vacuum region between the plasma and the outer radius R_w, the third term is the Poynting energy flux per unit length into the plasma plus vacuum region, and the terms on the right represent the $\mathbf{J}\cdot\mathbf{E}$ energy exchange rate per unit length within the plasma. The sum of eqn.(21) with eqn.(15) gives the the total plasma plus field energy equation:

$$\frac{d}{dt}\left(\frac{I^2}{c^2}\right) + \frac{d}{dt}\left[\frac{I^2}{c^2}\ln\left(\frac{R_w}{R_o}\right)\right] = IE_Z(R_w) - \frac{P_{rad}}{\Delta Z} \,. \tag{22}$$

This conservation relation shows that the rate of energy input to the system consisting of the plasma column and surrounding vacuum is $IE_Z(R_w)\Delta Z$. In turn,

this expression must be the rate of energy drawn off the generator circuit, and the load voltage drop is

$$\frac{V_{load}}{\Delta Z} = E_Z(R_w) = \left[\frac{1}{2c^2} + \frac{2}{c^2}\ln\left(\frac{R_w}{R_o}\right)\right]\frac{dI}{dt} + \left[-\frac{2}{c^2}\frac{V_o}{R_o} + \frac{\bar{\eta}_\perp}{\pi R_o^2}\right]I \ . \qquad (23)$$

The result on the right hand side comes from evaluating eqn.(21). The circuit eqn.(17) can now be written as

$$\left[\frac{L_g}{\Delta Z} + \frac{1}{2c^2} + \frac{2}{c^2}\ln\left(\frac{R_w}{R_o}\right)\right]\frac{dI}{dt} = \frac{V_g}{\Delta Z} - \left[\frac{Z_g}{\Delta Z} - \frac{2}{c^2}\frac{V_o}{R_o} + \frac{\bar{\eta}_\perp}{\pi R_o^2}\right]I \ . \qquad (24)$$

The generator inductance is enhanced by a small constant term and a motional inductance term given on the left of the above equation. In addition to the generator impedance one finds on the right of the above equation a motional impedance and a resistive impedance term.

D. Resistivity

Equations (16) and (24) are the basic equations for the radius and current in our model of the quasi-static Bennett pinch collapse. To solve these equations we must first specify the relations used for the electrical resistivity and radiative cooling loss. For the resistivity we employ the standard Spitzer formula[8]:

$$\eta_\perp = \frac{m_e}{e^2 n_e \tau_{ei}} = 1.14\times10^{-14}\,\frac{Z_i \ln(\Lambda_{ei})}{T_{eV}^{3/2}} \quad \text{sec} \ , \qquad (25)$$

where τ_{ei} is the electron-ion collision time[9] and $\ln(\Lambda_{ei})$ is the classical Coulomb logarithm for electron-ion collisions. We evaluate the Coulomb logarithm at the average column density for $\bar{\eta}_\perp$ in eqns.(16) and (24) above. At high densities the effects of electron degeneracy, strong coupling, and ion-ion correlations significantly change the electrical resistivity. For the present report these effects are neglected. The Coulomb logarithm is floored at 2.0 to prevent unphysical negative values for the resistivity.

E. Radiation Transport

For a deuterium z-pinch at temperatures above 10eV one can take the plasma to be fully ionized. Hence only free-free transitions occur with the Bremsstrahlung emissivity:

$$j_\nu = \frac{8}{3}\left(\frac{2\pi}{3}\right)^{1/2}\frac{e^6}{m_e^{3/2}c^2}\, g_{ff} n_e n_i \frac{e^{-h\nu/k_BT}}{(k_BT)^{1/2}} \quad , \tag{26}$$

where g_{ff} is the free-free Gaunt factor. If the plasma column were optically thin throughout its evolution, then the frequency and volume integral of j_ν would be the radiative loss term:

$$P_{rad}(thin) = \int_0^{R_o}\left(\int_0^{\infty} 4\pi j_\nu d\nu\right) 2\pi r dr dz$$

$$= \pi R_o^2 \Delta Z\, \frac{32\pi}{3}\left(\frac{2\pi}{3}\right)^{1/2}\frac{e^6}{m_e^{3/2}c^3h}\, \bar{n}_e \bar{n}_i Z_i \langle g_{ff}\rangle (k_BT)^{1/2}. \tag{27}$$

Here $\bar{n}_i$ and $\bar{n}_e$ are the mean ion and electron densities in the plasma column and $\langle g_{ff}\rangle$ is the frequency average of the Gaunt factor. For frequencies near the peak of the blackbody spectrum at temperatures between 0.1 and 10 keV the free-free Gaunt factor can be taken as unity[10].

We will find, however, that the plasma collapses to small enough radii that opacity effects become important. Since the radiation output from the dense z-pinch is of primary interest in the present report we must account for the opacity changes. For Bremsstrahlung absorption the coefficient is given by Kirchhoff's law $\kappa_\nu = j_\nu/B_\nu$, where B_ν is the Planck function:

$$\kappa_\nu = \frac{4}{3}\left(\frac{2\pi}{3}\right)^{1/2}\frac{e^6h^2}{m_e^{3/2}c}\,\frac{n_e n_i Z_i}{(k_BT)^{7/2}}\, g_{ff}\, \frac{1 - e^{-h\nu/k_BT}}{(h\nu/k_BT)^3} \quad . \tag{28}$$

The solution to the radiative transfer equation for the specific intensity at a point R_o on the surface of the plasma column in the ray direction Ω is

$$I_\nu(R_o,\Omega) = \int_0^{s(R_o,\Omega)} j_\nu e^{-\kappa_\nu s'} ds' = B_\nu\left(1 - e^{-\kappa_\nu s(R_o,\Omega)}\right) . \qquad (29)$$

Here $s(R_o,\Omega)$ is the path length through the plasma looking backwards along the ray Ω from the point R_o. To solve the radiative transfer problem for the dense z-pinch we will make several simplifying approximations. First, in addition to the uniform temperature in the plasma column, we take the plasma column to have a uniform density as given by the average value $N_1/\pi R_o^2$. From eqn.(7) only the outer 13% of the column differs by more than a factor of two from the average density. This approximation was used to obtain the last equality in the above equation. Second, we consider only a single ray along the diameter of the plasma column. Then $s(R_o,\Omega)$ reduces to $2R_o$. Third, we seek a frequency-averaged value for the opacity, $\kappa_\nu \rightarrow \bar{\kappa}$, such that the blackbody and optically thin limits are properly recovered. To this end note that the radiation loss rate of the plasma column is equal to the surface area times the radiative flux at the plasma surface in the radially outward direction:

$$P_{rad} = 2\pi R_o \Delta Z \int F_\nu d\nu = 2\pi R_o \Delta Z \int \left(\int \Omega\cdot e_R I_\nu d\Omega\right) d\nu$$

$$= 2\pi R_o \Delta Z \int \pi B_\nu \left(1 - e^{-\bar{\kappa} 2R_o}\right) d\nu = 2\pi R_o \Delta Z \sigma_{SB} T^4 \left(1 - e^{-\bar{\kappa} 2R_o}\right), \qquad (30)$$

where σ_{SB} is the Stefan-Boltzmann constant $= 2\pi^5 k_B^4/(15c^2h^3)$. In the optically thick limit ($\bar{\kappa}2R_o \rightarrow \infty$), P_{rad} obviously becomes the emission rate from a blackbody column. In the opposite limit, P_{rad} of eqn.(30) must reduce to P_{rad}(thin) of eqn.(27). This requires

$$\bar{\kappa} = \frac{4}{3}\left(\frac{2\pi}{3}\right)^{1/2} \frac{e^6 h^2}{m_e^{3/2} c} \frac{\bar{n}_e \bar{n}_i Z_i^2}{(k_B T)^{7/2}} \langle g_{ff} \rangle \frac{15}{\pi^4} . \qquad (31)$$

The effective opacity of eqn.(30) agrees with eqn.(27) evaluated at the non-dimensional frequency $h\nu/k_BT = 1.75$ in eqn.(27). For comparison, the peak of the blackbody spectrum occurs at $h\nu/k_BT = 2.82$.

The combination of eqns.(30) and (31) is in essence a probability of escape model for the radiation transport. This approach is both economical and reasonably accurate for calculating the effects on the dynamics due to radiative losses. However, this frequency-averaged approach provides no information on the shape of the emitted spectrum. For this reason a ray-trace code was developed which solved for the specific intensity of eqn.(29) at distinct frequencies by determining $s(R_o,\Omega)$ for a large number of ray directions. The results were then used to calculate the angle integral for the radiative flux of eqn.(30). Hence the frequency dependence of the radiative losses were determined exactly subject to the approximation of a uniform density and temperature plasma column. The details of the analysis will be presented in a later report on radiation from dense z-pinches. Due to the time consuming nature of the calculations, the ray-tracing code was employed only to postproccess a solution once the evolution of the radius and temperature were known.

III. RESULTS AND DISCUSSION

In order to solve eqns.(16) and (24) for the radius and current as a function of time we must first specify the parameters of the generator device and the initial conditions. We will present detailed results for a single run whose parameters are:

$$N_1 = 2.0\times10^{18}\ \text{cm}^{-1},$$

$$L_g = 100.0\ \text{nanohenries},$$

$$Z_g = 10^{-1}\ \text{ohms},$$

$$V_g = 500\ \text{kvolts},$$

$$R_w = 1.0\ \text{cm},$$

$$\Delta Z = 1.0\ \text{cm},$$

$$R_o(t=0) = 0.02 \text{ cm},$$

$$I(t=0) = 0.07 \text{ MA}. \qquad (32)$$

The starting conditions correspond to an initial temperature of 7.1 eV. The physics included in the present model is inadequate to correctly describe the cold start-up problem. Hence we chose an initial radius and temperature which could represent the state of the fiber after it has been substantially ionized and come into Bennett equilibrium. The simulation time t=0 is offset by an undetermined, but probably small, amount from the time of the circuit opening.

The time evolution of the radius, current and temperature are shown in Figs. 1a, 1b, and 1c, respectively. Blow-ups around the time of collapse for these same variables are displayed in Figs. 2a, 2b, and 2c.

As long as degeneracy effects are not significant and the ionization energy is constant, the Bennett relation [eqn.(10)] indicates that the internal energy and temperature are solely dependent upon the line density N_l, which is known, and the current I, which is found by solving eqn. 17. Since L_g is fixed and Z_g is negligible in eqn.(17), the current I can be determined if the voltage across the plasma load, V_{load}, is known. Until the time of dramatic plasma collapse, which begins at t ≈ 550 nsec, V_{load} is small compared to the machine parameter L_g. At this time the plasma inductance has reached about 1/8 of the machine inductance and the resistive and motional components of the plasma impedance are still negligible. Because all three components of V_{load} in eqn.(23) depend upon some function of R_o^{-1}, V_{load} only becomes significant late in the collapse phase of the implosion. Therefore, during the early stages of the implosion the current is practically independent of V_{load} and is given approximately by $I = (V_g/L_g)t$, where t is the elapsed time.

The early time expansion of the fiber radius can be explained by the fact that most of the electrical energy is initially going into charging the machine inductance rather then changing the internal energy of the fiber, i.e. $d/dt(3I^2/4c^2)$ is small in eqns.(15) and (16). Therefore the plasma expands or contracts according the to the relative strengths of ohmic heating and radiative cooling. In our case the plasma expands because ohmic heating is initially dominant. However, if we had chosen a larger driving voltage or smaller machine inductance, then the internal energy would initially increase

more rapidly. If it were fast enough, the increase could not be solely provided by ohmic heating but would have to be accompanied by contraction of the plasma in the form of P-d(volume) work. In this example, the rate of change of internal energy is sufficient at t = 20 nsec that the plasma starts to collapse.

At t = 320 nsec the the current has reached the "Pease-Braginskii" current, I_{PB} , i.e. the current at which the ohmic heating rate is equal to the radiative cooling rate. As the current is increased above I_{PB} the radiative cooling rate begins to dominate and further enhances the plasma collapse. This is a highly non-linear situation because, as the plasma collapses, the radiation rates go up as the density squared in the optically thin limit. Eventually, as the current continues to rise and the radius decreases the plasma impedance begins to influence the circuit. At t = 543 nsec the current begins to decrease because the plasma impedance has increased to the point that the voltage across the plasma, V_{load}, is now equal to the machine voltage, V_g.

After the peak in the current, radiative rates continue to dominate and drive the plasma to further collapse. The most dramatic stage of this collapse occurs at t = 554 nsec and lasts less than 1 nsec. The collapse is eventually stopped and the plasma begins to expand when the ohmic heating rate exceeds the opacity limited radiative rate. The opacity is so large at this stage, due to large densities, that the spectrum is nearly blackbody.

During the rapid collapse, electron degeneracy also indirectly contributes to limiting the plasma radius by lowering the overall temperature according to eqn.(10) This allows the ohmic heating rate to overtake the radiative cooling rate at a higher current than would occur without degeneracy effects. The importance of electron degeneracy is indicated by the large Fermi temperature that occurs at maximum compression as shown in Fig. 2c.

When the radius reaches its minimum value at $R_o \simeq 3 \times 10^{-5}$ cm (Figs. 1a and 2a) the current is still near peak value. However, the current quickly decays because the plasma impedance is now large, on the order of 100's of ohms, and therefore $V_{load} >> V_g$. Under these circumstances, the current decay is given to first approximation by,

$$dI/dt = - V_{load}/L_g$$

Although the internal energy decreases by a factor of 5, a difference of 2 kJ, during the final collapse, most of the energy that is radiated out of the system at this time is not the result of direct conversion of thermal energy. Instead it is supplied by the discharging magnetic field energy, which is stored in the inductive components of the machine and plasma, as the current decreases from 1.9 to .8 MA. This electrical energy is channeled into the plasma in the form of ohmic heating and P-d(volume) work and is quickly radiated out of the plasma. The integral of $L_g I(dI/dt)$ over the time interval from peak current until minimum current, $\simeq$ 5 nsec, reveals that there is over 150 kJ of energy discharged through the machine inductor. This does not take into account the additional magnetic energy discharged through the plasma.

The radiated power during the entire run is shown in Fig.3. The photon energy, E_γ, is divided into three bands; $E_\gamma<1$ keV, $1<E_\gamma<3$ keV, and $E_\gamma>3$ keV. One can clearly see the sharp spike in the radiated power denoting the collapse of the plasma column. Simple analysis of eqn.(22) shows that at the time of peak current, the radiative emission is limited to $IV_{load}\leq 1.0$ TW. However, as dI/dt becomes negative, the peak radiative power grows to ~100 TW, most of which is in the $E_\gamma>3$ keV energy range. A blow-up of the radiated power for the same energy bands as above over the temporal region around the collapse is given in Fig.4. The sudden drop in the power immediately following the peak in each band reflects the rapid decrease in the radius and temperature of the nearly blackbody plasma column. The spectral distribution of the emitted radiation is shown at three distinct times in Fig.5. The emission spectrum at the peak of the current (543 nsec) is presented in the left hand panel of Fig. 7; at the minimum radius of the collapse (554.8 nsec) in the center panel, and at the minimum current (564 nsec) in the right hand panel. The transition in the spectra from thin to thick, and back to partially thin during the collapse phase is evident. The time integral of the radiative output in the same three bands as above is displayed in Fig.6. About 100 kJ of radiation is produced with ~40% of the energy emitted as photons above 3 keV.

Finally, we again note that the radiation results displayed in this report are calculated by post processing the temperature and density profiles using the detailed ray-trace radiation transport model described earlier (§II.E). The calculation from which the temperature and density profiles were obtained assumed a frequency independent opacity according to eqn.(28). This was done in order to speed up the calculation but at the same time retain the

essential radiation physics. In general the results of the two calculations agree to well within a factor of two.

IV. CONCLUSION

The single example simulation was presented here more in the spirit of a "proof of principle" discussion rather than a complete and exact analysis of the dense z-pinch concept for a plasma radiation source. Taken at face value, the results of this one simulation does indicate that a dense z-pinch could produce over 40 kJ of photons, with energies exceeding 3 keV, in a 1 nsec time span. We conclude that a fiber z-pinch driven by a slowly rising current is a potentially robust plasma radiation source. We emphasize potentially robust, first of all, because of the need to verify the simple theoretical model used in the text. Several key issues associated with the rapid and strong collapse phase are currently under study. These include:

- a more rigorous inclusion of electron degeneracy effects on the electron pressure and internal energy instead of the simplified approximation used in eqn.(10);
- the inclusion of degeneracy and strong coupling effects on the Coulomb logarithm and resistivity to replace the Spitzer formula of eqn.(25);
- the reduction of Bremsstrahlung emission in eqn.(26) due to the cutoff of available states in a degenerate plasma;
- a determination of the regime wherein the Bennett pressure equilibrium condition remains valid;
- and finally a determination of the conditions which will maintain a uniform current density within the plasma.

Second, we emphasize potentially robust because experiments need to be run in order to obtain a better understanding of these pinches. Finally, the duration of the radiation pulse could potentially be increased above a nanosecond by arranging a set of dense z-pinches to collapse sequentially in

time. Perhaps the most important feature of the present study is that a keV photon energy source could be accomplished with present day technology machines.

ACKNOWLEDGEMENTS

The authors gratefully acknowledge several fruitful discussions with Dr. A. E. Robson which were instrumental in initiating this research. The work was sponsored in part by the Defense Nuclear Agency and by the Office of Naval Research.

REFERENCES

(1) J. D. Sethian, A. E. Robson, K. A. Gerber, and A. W. DeSilva, Phys. Rev. Lett., 59, 892 (1987). Errata: ibid. p.1790.

(2) J. E. Hammel and D. W. Scudder, Proc. 14th Europ. Conf. on Controlled Fusion and Plasma Physics, Madrid 1987, Contributed Papers, Pt. 2 (EPS 1987), p.450.

(3) W. H. Bennett, Phys. Rev., 45, 890 (1934); J. A. Bettencourt, Fundamentals of Plasma Physics, (Pergammon Press: New York, 1986), p.339.

(4) S. J. Stephanakis, J. P. Apruzese, P. G. Burkhalter, J. Davis, R. A. Meger, S. W. McDonald, G. Mehlman, P. F. Ottinger, and F. C. Young, Appl. Phys. Lett., 48, 829 (1986).

(5) J. P. Apruzese and J. Davis, NRL Memorandum, 5406, (1984).

(6) N. R. Pereira and J. Davis, J. Appl. Phys., 64, R1, (1988).

(7) R. S. Pease, Proc. Phys. Soc., B70, 11 (1957); S. I. Braginskii, Sov. Phys. JETP, 6, 494 (1958).

(8) L. Spitzer, Jr., Physics of Fully Ionized Gases, 2nd Ed., (Interscience Publishers: New York, 1962), p.136.

(9) S. I. Braginskii, Reviews of Plasma Physics, Vol. I (Consultants Bureau, New York, 1965), p.205.

(10) W. J. Karzas and R. Latter, Astrophys. J., Suppl., 6, 167 (1961).

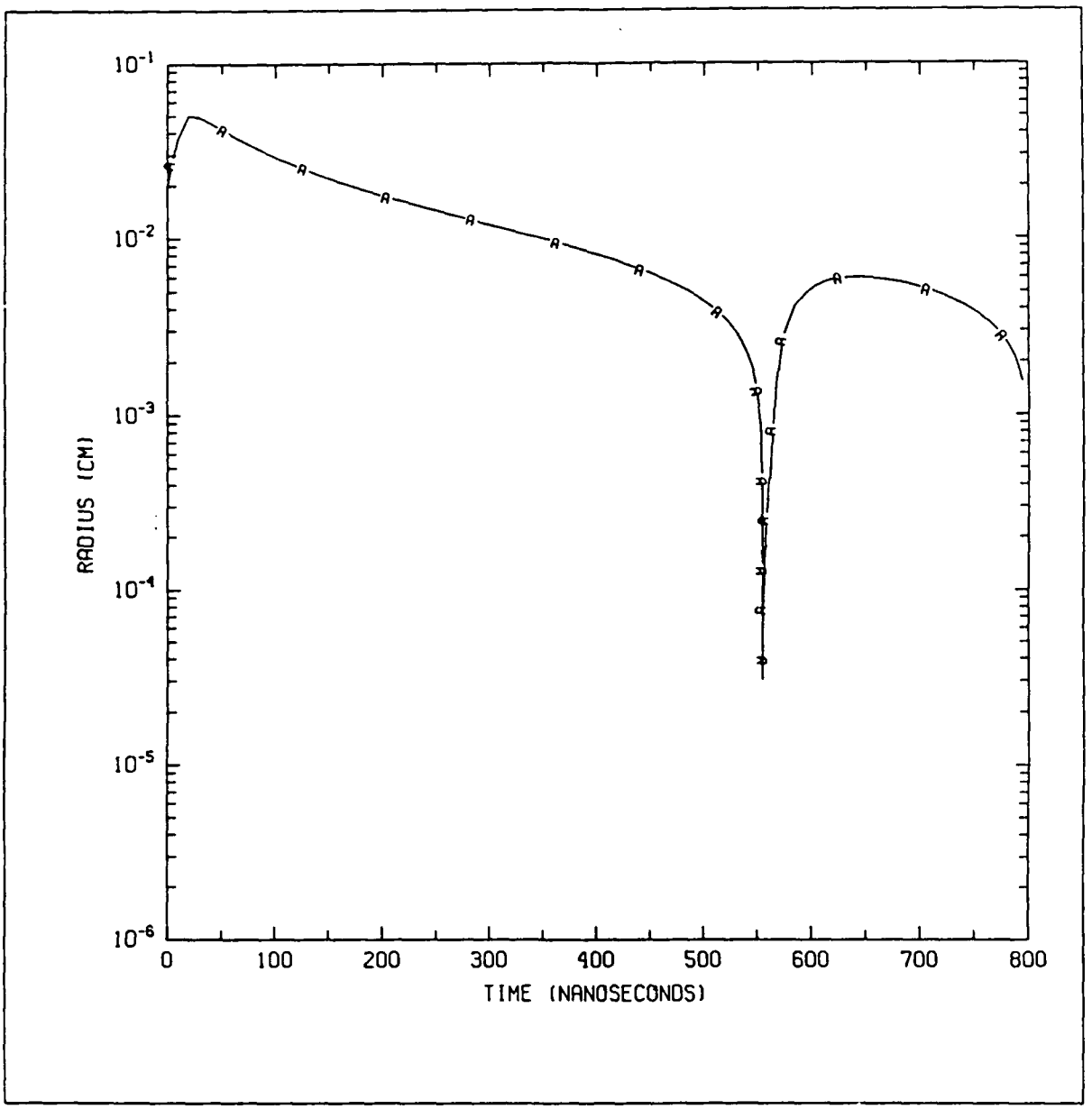

Fig.1a Temporal evolution of the radius for the model parameters given by eqn.(32) of the text.

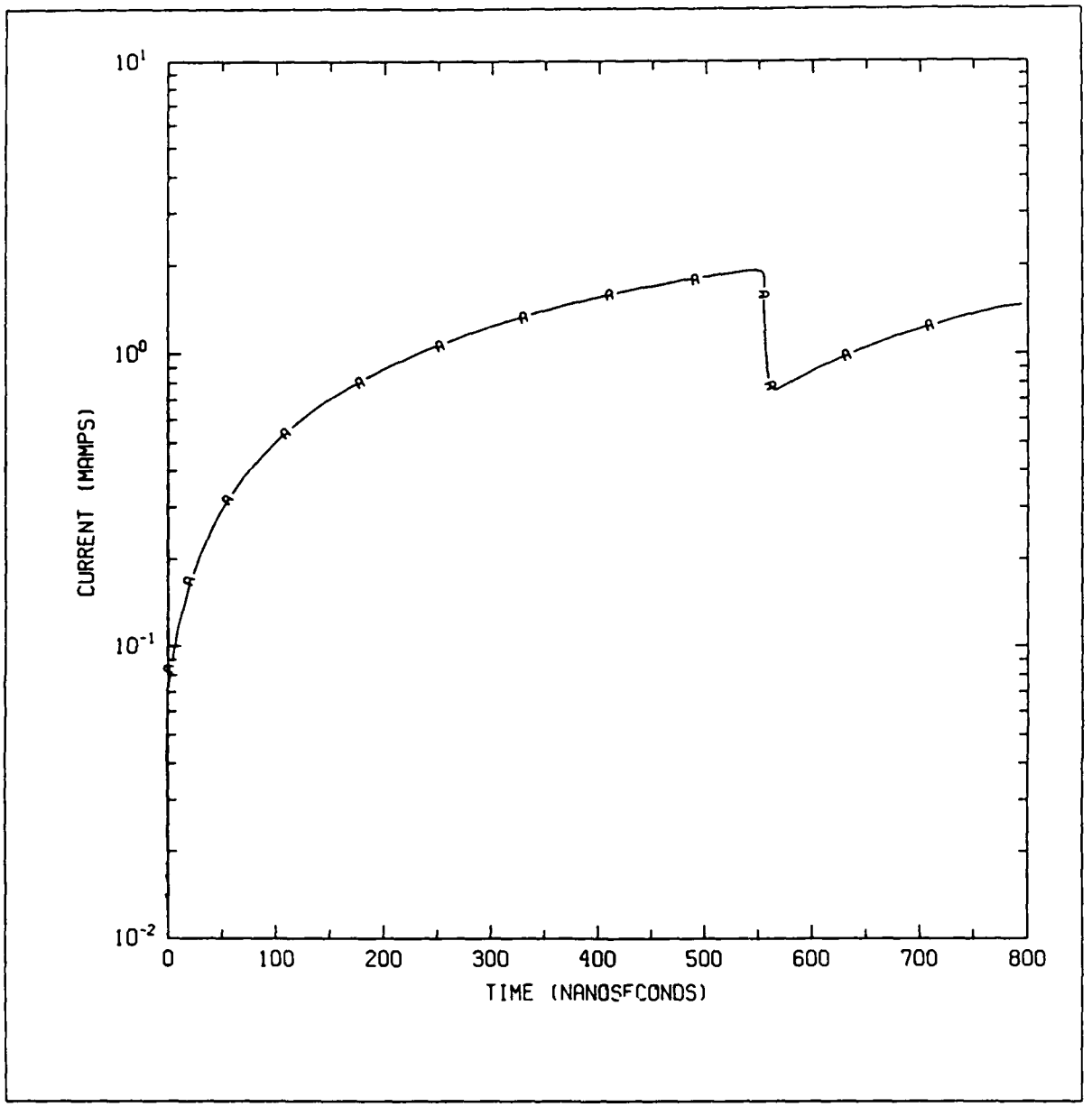

Fig.1b Temporal evolution of the current for the model parameters given by eqn.(32) of the text.

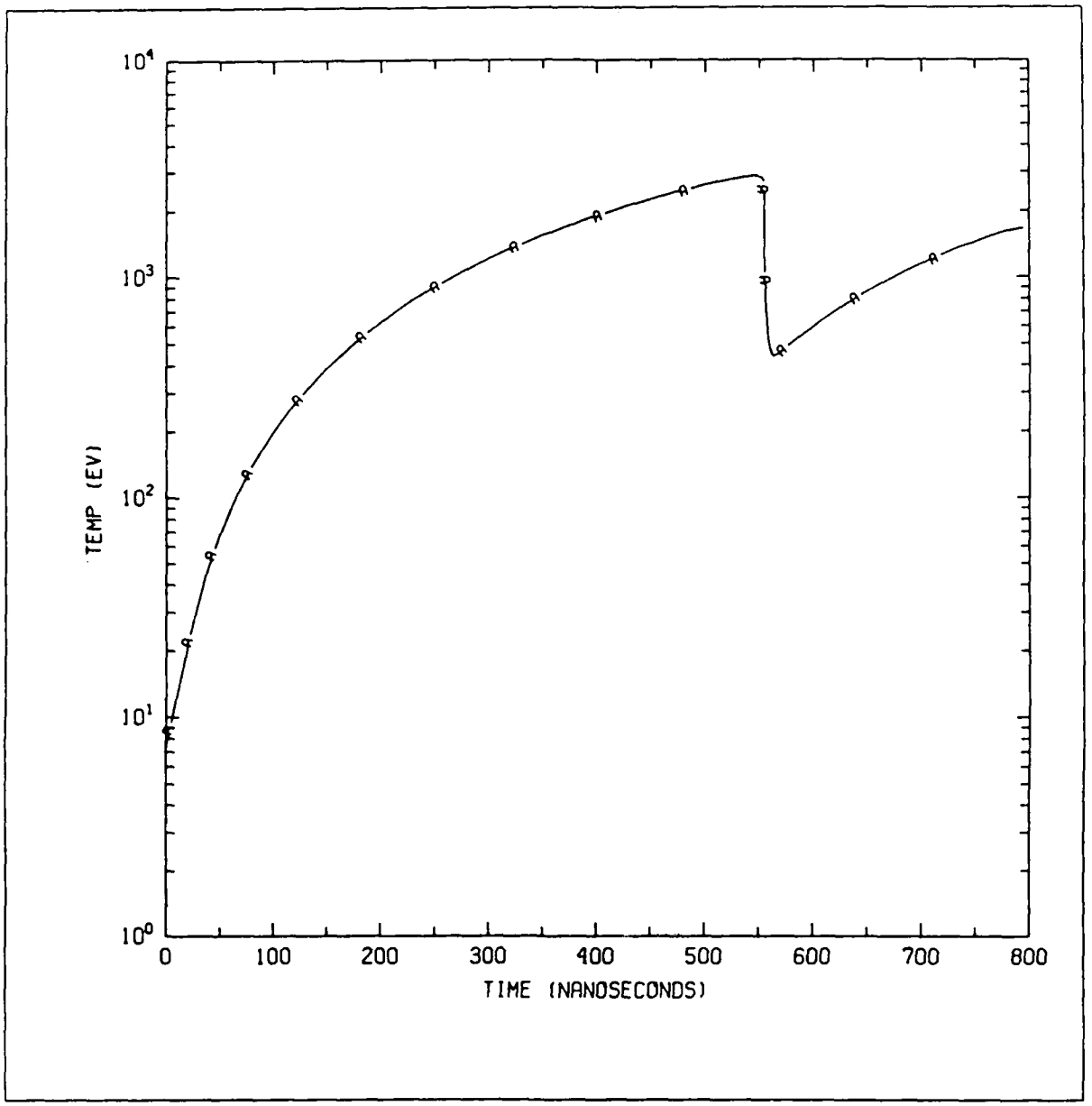

Fig.1c Temporal evolution of the temperature for the model parameters given by eqn.(32) of the text.

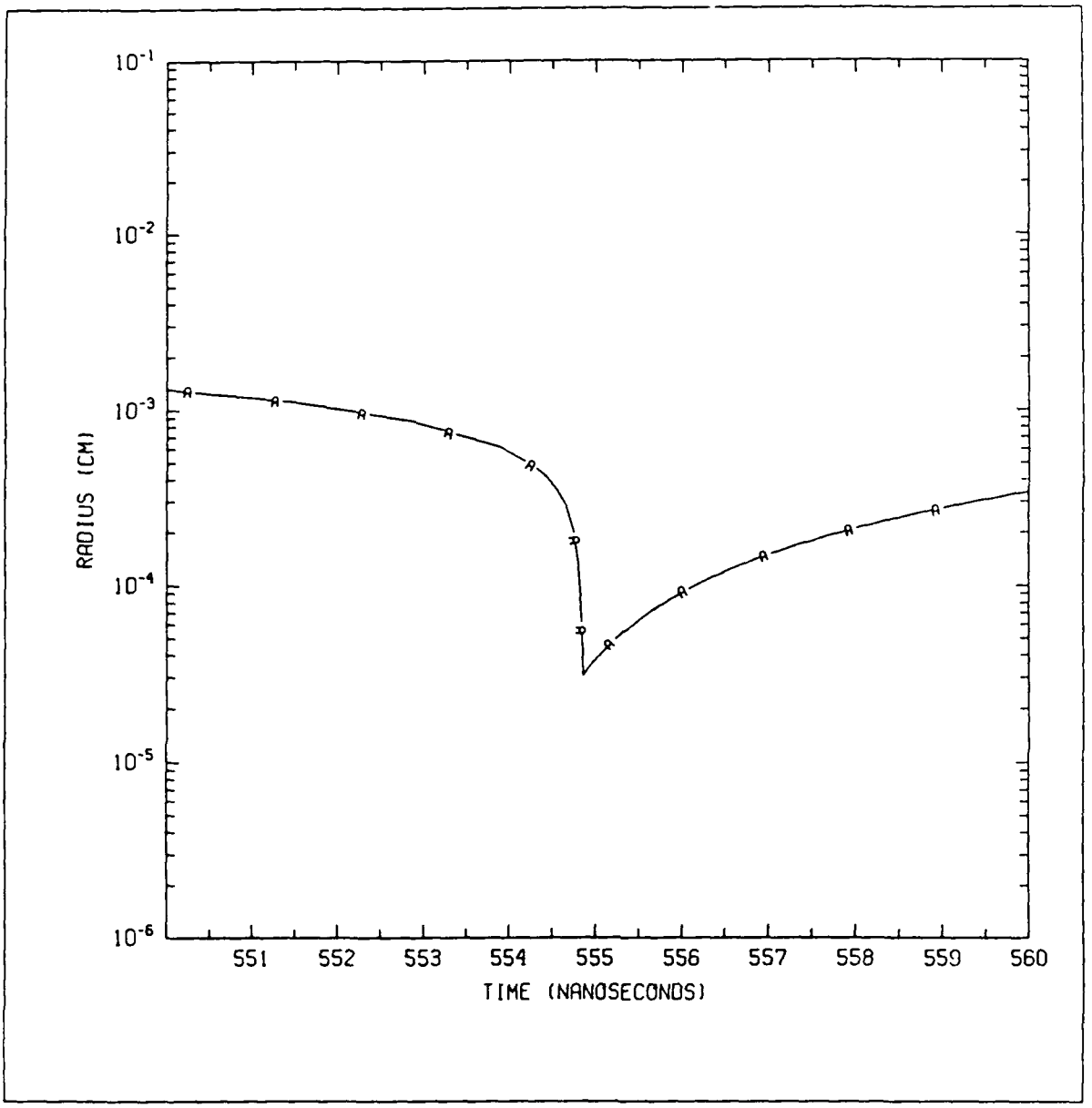

Fig.2a Blow-up of the temporal evolution of the radius during the rapid collapse phase of the implosion.

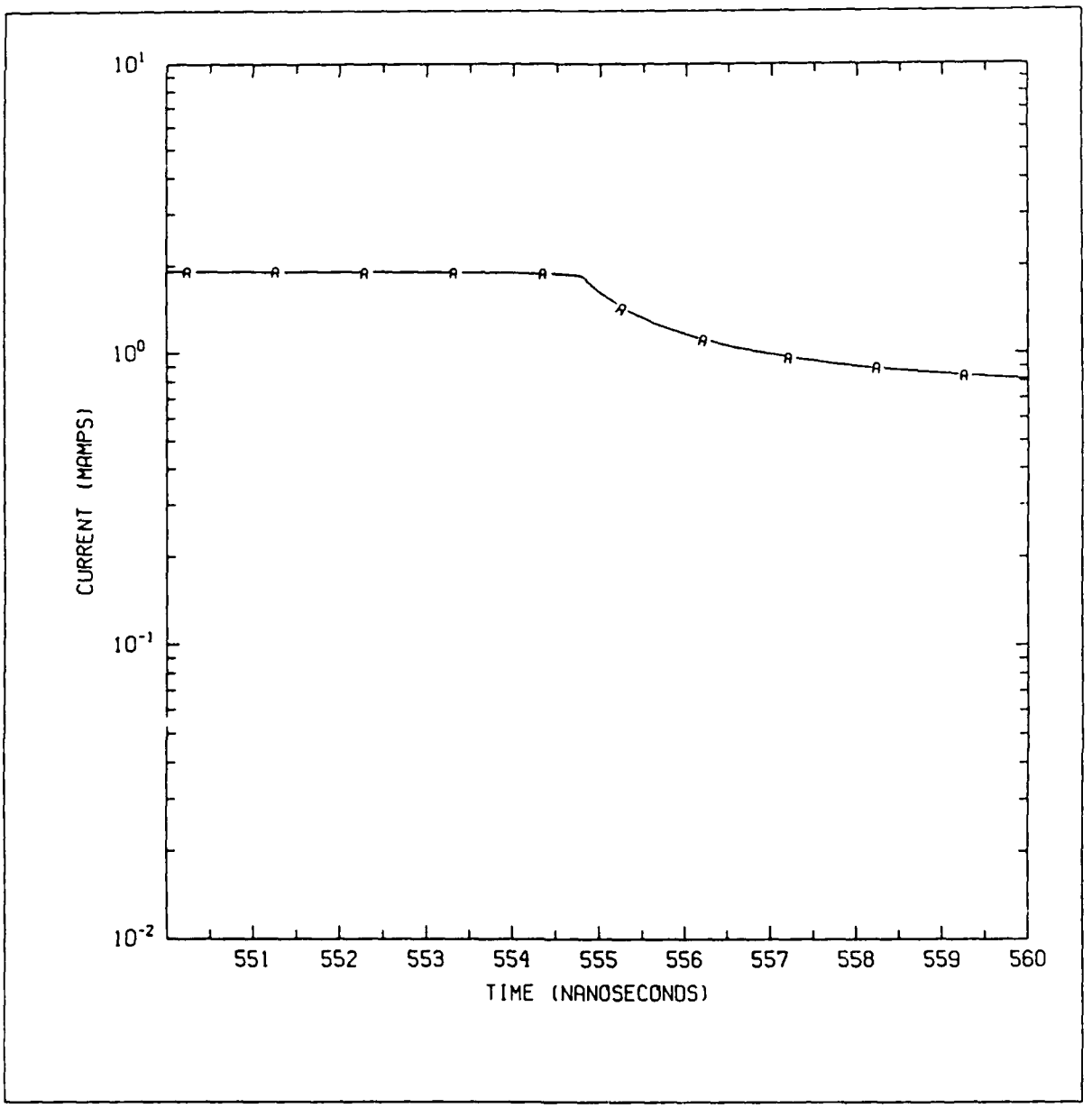

Fig.2b Blow-up of the temporal evolution of the current during the rapid collapse phase of the implosion.

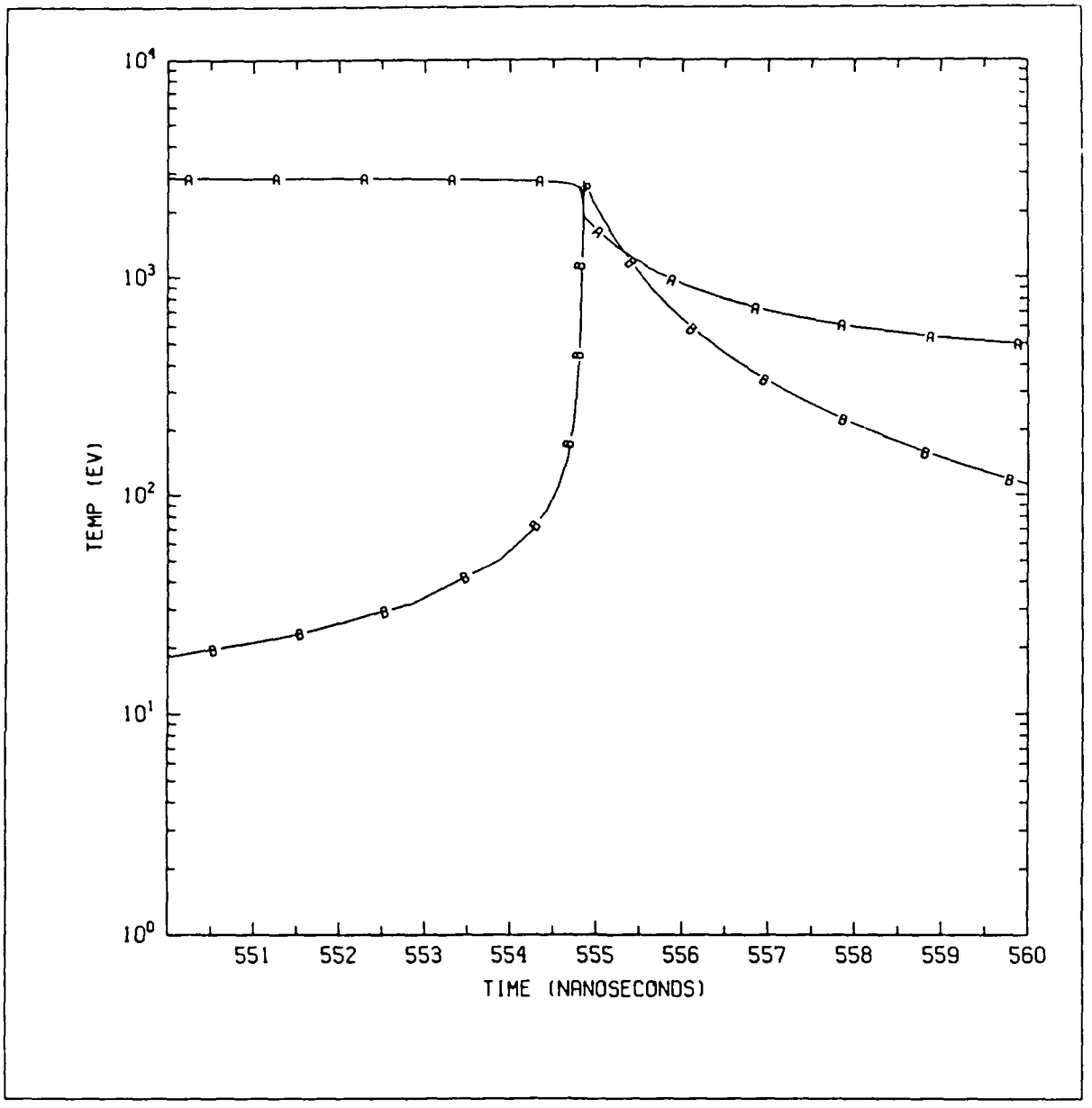

Fig.2c Blow-up of the temporal evolution of the temperature during the rapid collapse phase of the implosion. The thermal temperature is denoted by the A-line, and the Fermi temperature by the B-line.

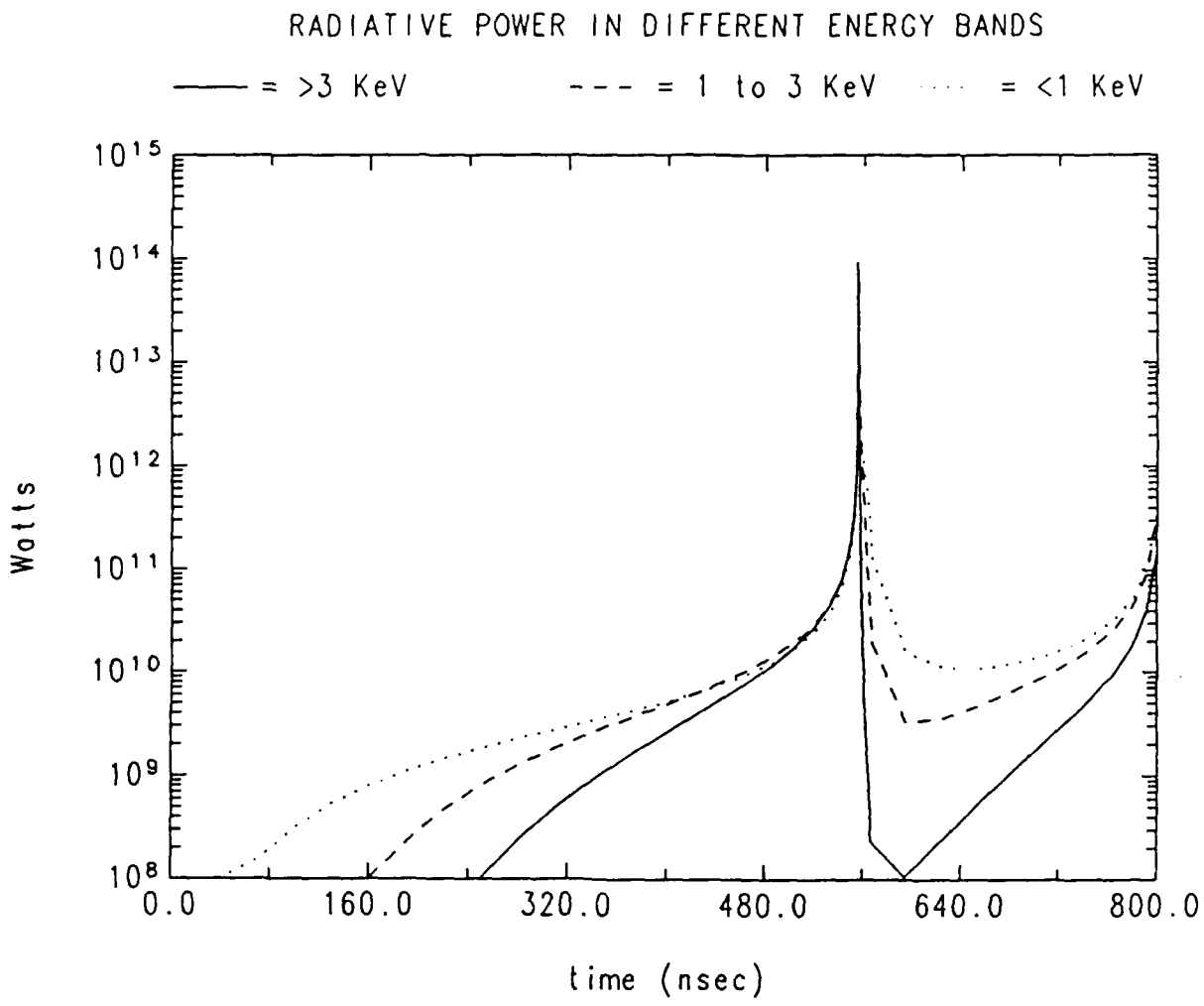

NLINE (cm^{-1})	LG (nhenrys)	ZG (ohms)	VG (kvolts)	RW (cm)	ΔZ (cm)	ROO (cm)	ICURNTO (MA)
2.00E+18	1.00E+02	1.00E-01	5.00E+02	1.00E+00	1.00E+00	2.00E-02	.14E-02

Fig.3 Temporal evolution of the radiative power in different energy bands for the model parameters given by eqn.(32) of the text.

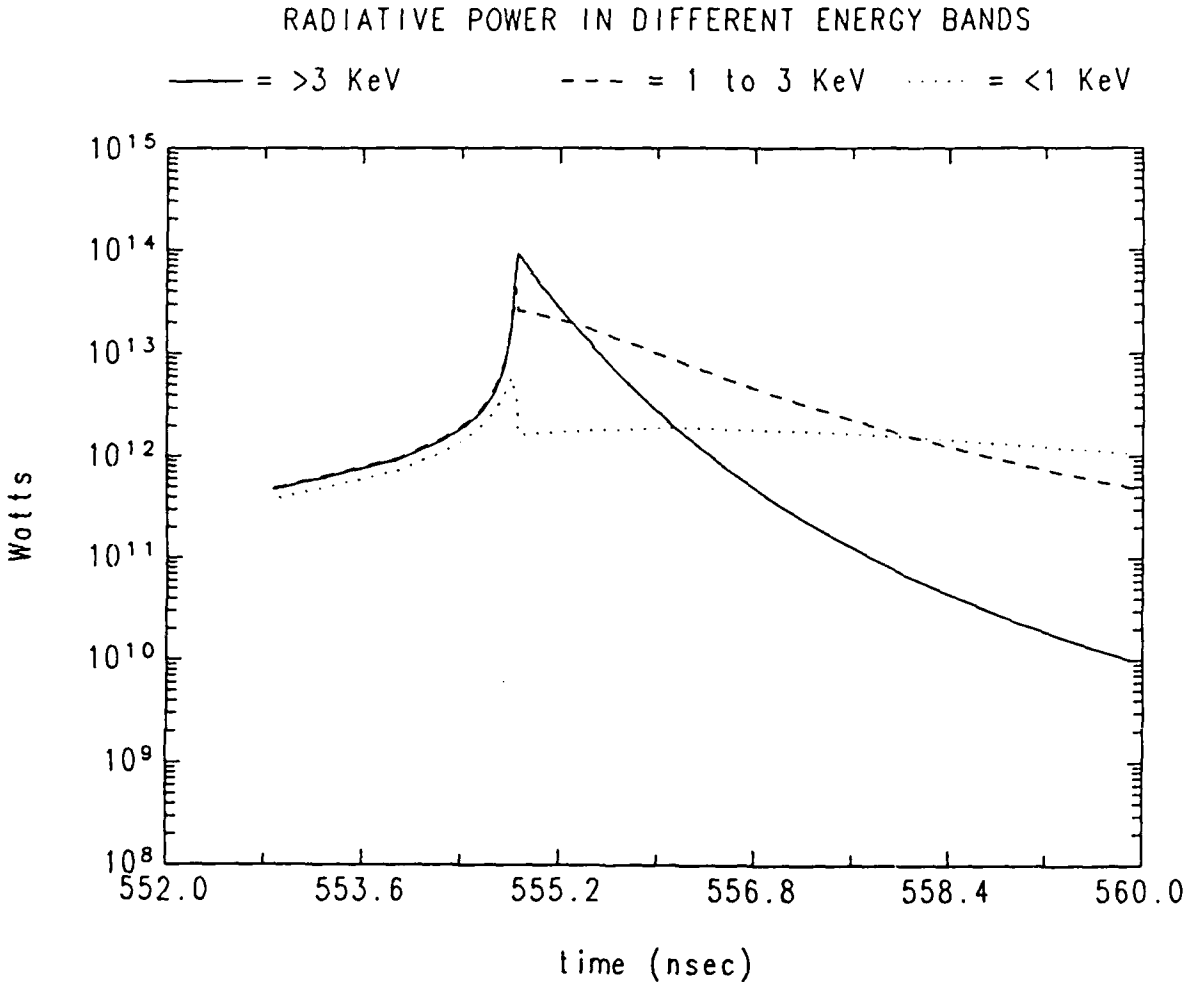

NLINE	LG	ZG	VG	RW	ΔZ	ROG	ICURNTO
(cm^{-1})	(nhenrys)	(ohms)	(kvolts)	(cm)	(cm)	(cm)	(MA)
2.00E+18	1.00E+02	1.00E-01	5.00E+02	1.00E+00	1.00E+00	2.00E-02	7.14E-02

Fig.4 Blow-up of the temporal evolution of the radiative power in different energy bands during the rapid collapse phase of the implosion.

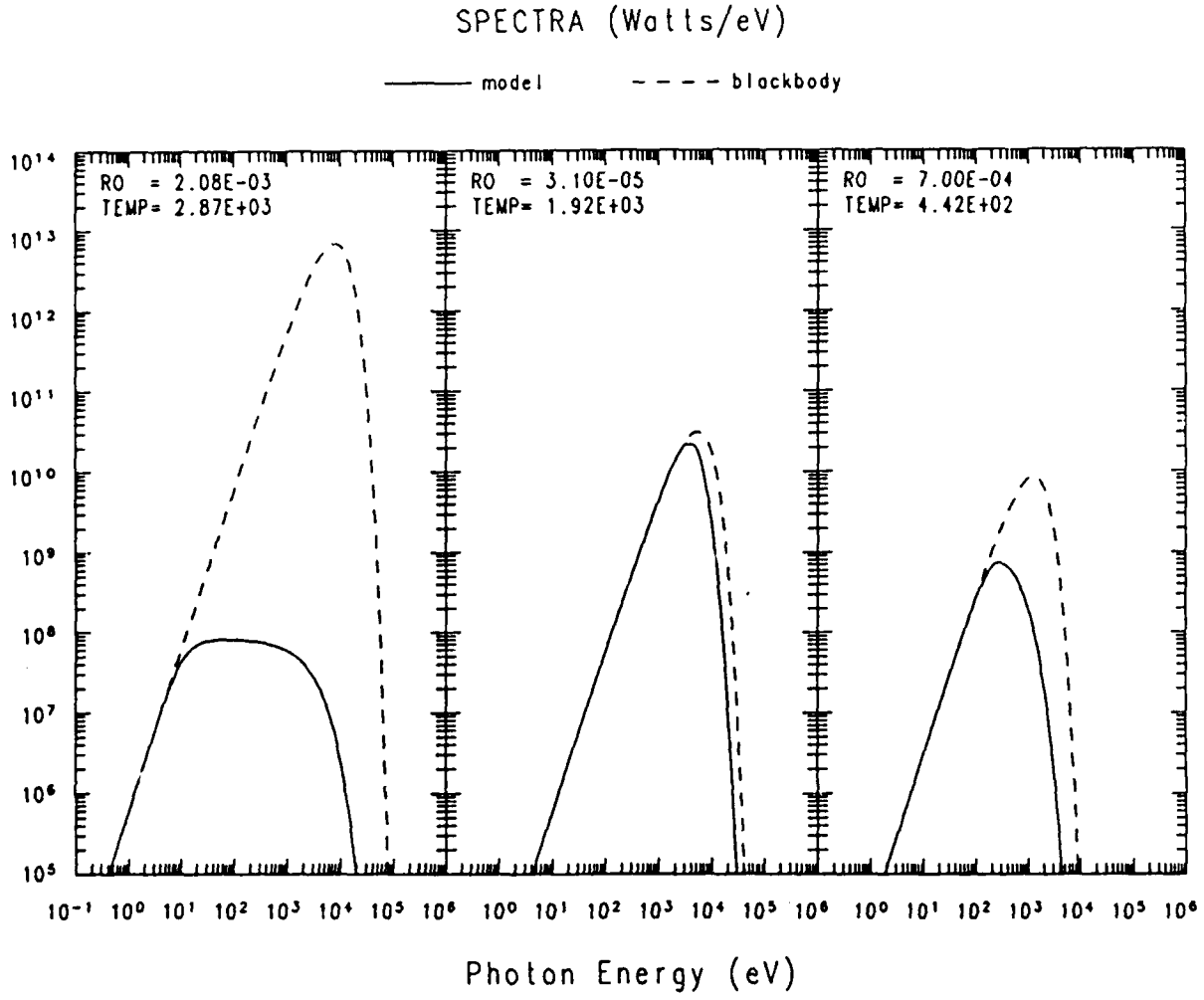

NLINE (cm^{-1})	LG (nhenrys)	ZG (ohms)	VG (kvolts)	RW (cm)	ΔZ (cm)	ROO (cm)	ICURNTO (MA)
2.00E+18	1.00E+02	1.00E-01	5.00E+02	1.00E+00	1.00E+00	2.00E-02	7.14E-02

Fig.5 Spectra of the radiative emission at the time of peak current (a), at the time of peak compression during the collapse (b), and at the time of minimum current (c).

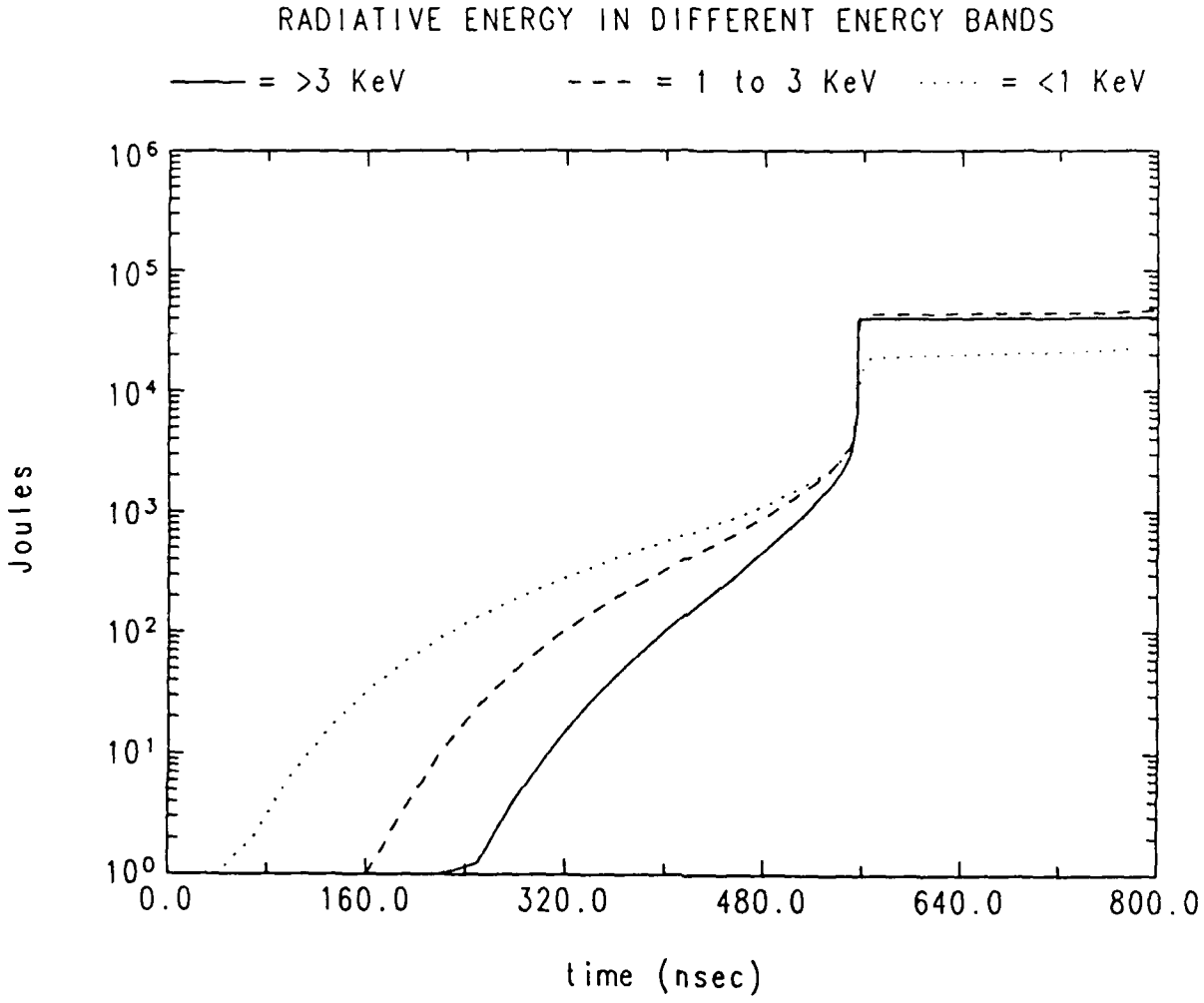

NLINE	LG	ZG	VG	RW	ΔZ	RO
(cm^{-1})	(nhenrys)	(ohms)	(kvolts)	(cm)	(cm)	(cm)
2.00E+18	1.00E+02	1.00E-01	5.00E+02	1.00E+00	1.00E+00	2.00E-02

Fig.6 Temporal evolution of the radiated energy in different energy bands.

DISTRIBUTION LIST

Assistant to the Secretary of Defense Atomic Energy Washington, D.C. 20301 Attn: Executive Assistant	1 copy
Director Defense Nuclear Agency Washington, D.C. 20305	
Attn: DDST	1 copy
TITL	4 copies
RAEV	1 copy
STVI	1 copy
Commander Field Command Defense Nuclear Agency Kirtland AFB, New Mexico 87115 Attn: FCPR	1 copy
Chief Field Command, Livermore Division Department of Defense Post Office Box 808 Livermore, California 94550 Attn: FCPRL	1 copy
Director Joint Strat TGT Planning Staff Offutt AFB Omaha, Nebraska 68113 Attn: JLKS	1 copy
Undersecretary of Defense for RSCH and ENGRG Department of Defense Washington, D.C. 20301 Attn: Strategic and Space Systems (OS)	1 copy
Deputy Chief of Staff for RSCH DEV and ACQ Department of the Army Washington, D.C. 20301 Attn: DAMA-CSS-N	1 copy
Commander Harry Diamond Laboratories Department of the Army 2800 Powder Mill Road Adelphi, Maryland 20783 Attn: DELHD-N-NP	1 copy each
DELHD-R J. Rosado	
DELHD-TA-L (Tech. Lib.)	

U.S. Army Missile Command — 3 copies
Redstone Scientific Information Center
Attn: DRSMI-RPRD(Documents)
Redstone Arsenal, Alabama 35809

Commander — 1 copy
U.S. Army Nuclear and Chemical Agency
7500 Backlick Road
Building 2073
Springfield, Virginia 22150
Attn: Library

Commander — 1 copy
Naval Intelligence Support Center
4301 Suitland Road, Bldg. 5
Washington, D.C. 20390
Attn: NISC-45

Commander — 1 copy
Naval Weapons Center
China Lake, California 93555
Attn: Code 233 (Tech. Lib.)

Officer in Charge — 1 copy each
White Oak Laboratory
Naval Surface Weapons Center
Silver Spring, Maryland 20910
Attn: Code R40
Code F31

Air Force Weapons Laboratory — 1 copy each
Kirtland AFB, New Mexico 87117
Attn: Dr. William Baker
SUL
CA

Deputy Chief of Staff — 1 copy
Research, Development and Accounting
Department of the Air Force
Washington, D.C. 20330
Attn: AFRDQSM

Commander — 1 copy
U.S. Army Test and Evaluation Command
Aberdeen Proving Ground, Maryland 21005
Attn: DRSTE-EL

Auburn University
Department of Physics
Attn: Dr. J. Perez
Auburn, Al 36849

1 copy

AVCO Research and Systems Group
201 Lowell Street
Wilminton, Massachusetts 01887
Attn: Library A830

1 copy

BDM Corporation
7915 Jones Branch Drive
McLean, Virginia 22101
Attn: Corporate Library

1 copy

Berkeley Research Associates
Post Office Box 983
Berkeley, California 94701
Attn: Dr. Joseph Workman

1 copy

Berkeley Research Associates
Post Office Box 852
5532 Hempstead Way
Springfield, Virginia 22151
Attn: Dr. Joseph Orens

1 copy each

Boeing Company
Post Office Box 3707
Seattle, Washington 98134
Attn: Aerospace Library

1 Copy

The Dikewood Corporation
1613 University Blvd., N.E.
Albuquerque, New Mexico 87110
Attn: L. Wayne Davis

1 copy

General Electric Company - Tempo
Center for Advanced Studies
816 State Street
Post Office Drawer QQ
Santa Barbara, California 93102
Attn: DASIAC

1 Copy

Institute for Defense Analyses
1801 N. Beauregard Street
Alexandria, Virginia 22311
Attn: Classified Library

1 copy

IRT Corporation
Post Office Box 81087
San Diego, California 92138
Attn: R. Mertz

1 copy

JAYCOR — 1 copy
1608 Spring Hill Road
Vienna, Virginia 22180
Attn: R. Sullivan

JAYCOR — 1 copy
11011 Forreyane Road
Post Office Box 85154
San Diego, California 92138
Attn: E. Wenaas
F. Felbar

KAMAN Sciences Corporation — 1 copy each
Post Office Box 7463
Colorado Springs, Colorado 80933
Attn: Library

Lawrence Livermore National Laboratory — 1 copy each
University of California
Post Office Box 808
Livermore, California 94550
Attn: DOC CDN for 94550
DOC DCN for L-47 L. Wouters
DOC CDN for Tech. Infor. Dept. Lib.

Lockheed Missiles and Space Company, Inc. — 1 copy each
Post Office Box 504
Sunnyvale, California 94086
Attn: S. Taimlty
J.D. Weisner

Maxwell Laboratory, Inc. — 1 copy ea.
9244 Balboa Avenue
San Diego, California 92123
Attn: A. Kolb
M. Montgomery
J. Shannon
K. Ware

McDonnell Douglas Corporation — 1 copy
5301 Bolsa Avenue
Huntington Beach, California 92647
Attn: S. Schneider

Mission Research Corporation — 1 copy each
Post Office Drawer 719
Santa Barbara, California 93102
Attn: C. Longmire

Mission Research Corporation-San Diego — 1 copy
5434 Ruffin Road
San Diego, California 92123
Attn: Victor J. Van Lint

Northrop Corporation — 1 copy
Northrop Research & Technology Center
1 Research Park
Palos Verdes Peninsula, California 90274

Physics International Company — 1 copy each
2700 Merced Street
San Leandro, California 94577
Attn: M. Krishnan
C. Denney
T. Nash

R and D Associates — 1 copy each
Post Office Box 9695
Marina Del Rey, California 90291
Attn: Library

Sandia National Laboratories — 1 copy each
Post Office Box 5800
Albuquerque, New Mexico 87115
Attn: Doc Con For 3141
D. McDaniel
P. VanDevender
K. Matzen, Code 4247

Science Applications, Inc. — 1 copy
10260 Campus Point Drive
Mail Stop 47
San Diego, California 92121
Attn: R. Beyster

Spectra Technol, Inc., — 1 copy
2755 Northup Way
Bellevue, Washington 98004
Attn: Alan Hoffman

Spire Corporation — 1 copy
Post Office Box D
Bedford, Massachusetts 07130
Attn: R. Little

S-CUBED — 1 copy
Post Office Box 1620
La Jolla, California 92038
Attn: A. Wilson

Director — 1 copy each
Strategic Defense Initiative Organization
Pentagon 20301-7100
Attn: DE Lt. Col Richard Gullickson/DEO
IST Dr. Dwight Duston
IST Dr. Jonathan Farber

Texas Tech University — 1 copy
Post Office Box 5404
North College Station
Lubbock, Texas 79417
Attn: T. Simpson

TRW Defense and Space Systems Group — 1 copy
One Space Park
Redondo Beach, California 90278
Attn: Technical Information Center

Naval Research Laboratory
Plasma Radiation Branch
Washington, D.C. 20375
Code 4720 - 50 copies
4700 - 26 copies
2628 - 22 copies